Fluxon dynamics of a long Josephson junction with two-gap superconductors

Ju H. Kim, Bal-Ram Ghimire, and Hao-Yu Tsai

Phys. Rev. B **85**, 134511 — Published 12 April 2012

DOI: 10.1103/PhysRevB.85.134511

Fluxon Dynamics of a Long Josephson Junction with Two-gap Superconductors

Ju H. Kim, Bal-Ram Ghimire and Hao-Yu Tsai
Department of Physics and Astrophysics, University of North Dakota, Grand Forks, ND 58202-7129

We investigate the phase dynamics of a long Josephson junction (LJJ) with two-gap superconductors. In this junction, two channels for tunneling between the adjacent superconductor (S) layers as well as one interband channel within each S layer are available for a Cooper pair. Due to the interplay between the conventional and interband Josephson effects, the LJJ can exhibit unusual phase dynamics. Accounting for excitation of a stable 2π-phase texture arising from the interband Josephson effect, we find that the critical current between the S layers may become both spatially and temporally modulated. The spatial critical current modulation behaves as either a potential well or barrier, depending on the symmetry of superconducting order parameter, and modifies the Josephson vortex trajectories. We find that these changes in phase dynamics result in emission of electromagnetic waves as the Josephson vortex passes through the region of the 2π-phase texture. We discuss the effects of this radiation emission on the current-voltage characteristics of the junction.

PACS numbers: 74.20.De, 74.50.+r, 74.78.Fk, 85.25.Cp

I. INTRODUCTION

Recently discovered[1] iron-based superconductors have renewed much interest in the Josephson tunnel junctions involving multi-gap superconductors.[2,3] Both experimental and theoretical studies indicate that several other superconductors, including MgB_2,[4,5] $NbSe_2$,[6] heavy fermion UPt_3,[7] organic[8] $(TMTSF)_2X$ and $\kappa - BEDT$, may have multiple pesudo-order parameters. As the appearance of a phase texture and unusual Abrikosov vortex properties[9] in two-gap superconductors are considered as manifestations of the multi-component order parameter, the tunneling property of a Josephson junction with these superconductors may exhibit important differences from that with one-gap superconductors. This difference is attributed to the two tunneling channels for electrons in two-gap superconductor junctions due to the presence of two condensates. This internal freedom reflects the number of electronic bands participating in superconductivity. Consequently, dynamics of the relative phase of the order parameters for the two-gap superconductor tunnel junction differ from that of the one-gap superconductor junction.

The presence of two tunneling channels indicates that there are two types of relative phase dynamics in a long Josephson junction (LJJ) with two-gap superconductors. These phase dynamics may be understood in terms of the interplay between the interband and conventional (intraband) Josephson effects. The interband Josephson effect describes tunneling between two electronic bands in each superconductor (S) layer. On the other hand, the conventional Josephson effect describes tunneling between two adjacent S layers. These effects determine the dynamics of the phase difference between the condensates within the same S layer and across two adjacent S layers, respectively.

The relative phase of the two condensates is fixed in the ground state. This relative phase is locked to the value of 0 and π when the order parameter symmetry is S_{++} and S_{+-}, respectively. However, when the fluctuations about these phase-locked states are small, the interplay between the two Josephson effects can yield interesting phenomena. One such example is a collective excitation[3] known as Josephson-Leggett (JL) mode. This JL mode had been observed[10] in MgB_2 by Bloomberg and coworkers, using Raman scattering. Also, theoretical studies of superconductor-insulator-superconductor junctions between one- and two-gap superconductors suggest that the ground state may violate[11] the time reversal symmetry and that the phase dynamics of LJJ may depend on the symmetry of the superconducting order parameter.[12,13] This hetero-Josephson junction may be fabricated[14] by using Nb (one-gap) and either MgB_2 or iron-based superconductors (two-gap). Ota and coworkers suggested that the gap symmetry can affect[12] the Josephson current across the grain boundaries in polycrystalline samples as well as the current-voltage (I-V) characteristics of the multi-gap intrinsic LJJ stacks. Recent theoretical studies of hetero-Josephson junction suggest that the phase dynamics of LJJ are affected by the JL mode. The effects due to availability of two tunneling channels in LJJ may appear in measurable physical quantities, including the drastic enhancement of the macroscopic quantum tunneling rate and the presence of an extra step structure,[15] in addition to the conventional Shapiro steps, in the I-V characteristics.

A deviation from the phase-locked state in LJJ may not be limited to a small amplitude. The experimental data from the magnetic response of a superconducting ring with two pseudo-order parameters indicate that a stable soliton-shaped phase difference between the two condensates (i.e., i-soliton) is attainable.[16] This observation is consistent with a suggestion that the phase fluctuations can grow and produce a stable 2π-phase texture.[17] Excitation of i-soliton represents large phase fluctuations due to the interband Josephson effect and is taken as a hallmark of the multi-gap superconductors.

Soliton states in two-gap superconductors had been explored by a number of authors. Kupulevaksky and coworkers examined[18] this soliton state in mesoscopic thin-walled cylinders in external magnetic fields by using the Ginzberg-Landau approach,. Tanaka and coworkers suggested[19] that interesting excitations, including a phase domain surrounded by the i-soliton wall, can arise in two dimensions (i.e., D=2) since an i-soliton may be considered as a D-1 dimensional quantum phase dislocation. The i-soliton wall may carry a fractional flux quantum when one end of the soliton wall is terminated by the fractional vortex[9] while the other end is attached to a sample edge. Also, a vortex-molecule may be formed[20] when two fractional vortices, with a unit fluxoid quantum as the total magnetic flux, are connected by the i-soliton bond. These fractional vortices have been observed in a multi-layered superconductor[21] by using both magnetic force and scanning Hall probe microscopy.

The i-solitons differ from the Josephson vortices (i.e., fluxons) since they do not carry magnetic flux and do not interact with either magnetic field or supercurrents. However, an i-soliton may be formed and driven[22] by nonequilibrium charge density or by sufficiently strong superconducting currents. Gurevich and Vinokur suggested[22] that spontanteous apprearance of a soliton-like phase texture represents the breakdown of the phase-locked state. This breakdown can arise when the applied current density along the superconductor layers exceeds the critical value. The phase fluctuations may appear as either an additional resonances in the AC Josephson effect or a static 2π-kink in the phase difference. If the 2π-phase texture exists in each S layer, then this i-soliton may change the phase dynamics of the LJJ by inducing a critical current density modulation.

Earlier studies on the effects of critical current modulation indicate that both spatial and temporal dependence of Josephson current amplitude may be obtained by using experimental techniques such as Ohmic heating, quasiparticle injection, and illumination with an intensity modulated beam of light.[23] Also, a spatially periodic modulation of the critical current may be obtained from a periodic array of microresistors in the I layer.[24] As the microresistors behave as pinning centers for moving Josephson vortices (i.e., fluxons), the speed of the fluxon becomes modulated near each microresistor. The effects of a small periodic critical current modulation[23,25–27] created by an array of microresistors can yield a number of interesting properties, including emission of electromagnetic (EM) radiation and Josephson steps in the I-V characteristics.[23,25] This suggests that the spatial and temporal periodic modulation of the critical current due to excitation of the i-solitons may exibit the same interesting property.

Emission of EM radiation from an inhomogenous LJJ had been studied by using a number of different theoretical approaches, including Green function perturbation technique,[25] inverse scattering perturbation theory[26] and numerical simulation.[27] These studies reveal that a moving fluxon can radiate EM waves when its speed is larger than the critical value v_{th}. Also, the interference between the emitted EM waves can give rise to well-discernible steps in the I-V characteristics. This suggests that, if the critical current modulation is generated by large amplitude fluctuations of the phase difference, this may affect the junction property through the changes in the phase dynamics. These changes may be measured from the I-V curves. However, the effects of the interband Josephson current on the phase dynamics of a LJJ with two-gap superconductors have not yet been explored.

In this paper, we consider a quasi-one dimensional LJJ (i.e. D=1) with the dimensions, compared to the Josephson length λ_J, of $L_x \gg \lambda_J$ and $L_y \ll \lambda_J$ (see Fig. 1). We assume that there are no fractional vortices and investigate the effects of large phase functuations (i.e., i-soliton) on the phase dynamics of the LJJ. We note that, here, a weak external magnetic field, applied parallel to the insulator layer, penetrates the junction in the form of fluxons. Before proceeding further, we outline the main result. We find that i) large fluctuations in the relative phase of the two condensates in each S layer via the interband Josephson effect may be described by the sine-Gordon equation. ii) The soliton-like excitation (i.e., 2π-phase texure) can generate both a spatial and temporal modulation of the critical current between the adjacent S layers. iii) The critical current modulation yields emission of EM waves which radiate along the junction layer in a form of quasi-linear wave. The strength of the critical modulation is characterized in the I-V curve as a discontinous structure.

The outline of the remainder of the paper is as follows. In Sec. II, we describe the phase dynamics of a LJJ with two-gap superconductors by using a set of two sine-Gordon equations. In Sec. III, we derive the equation of motion for the relative phase of the two condensates in each S layer. In Sec. IV, we discuss the effects of the interband Josephson current on the phase dynamics by computing the radiation correction to the bare soliton solution. In Sec. V, we compute the trajectories of fluxon in the velocity-position phase plane and calculate the current-voltage characteristic curves. Finally, we summarize the result and conclude in Sec. VI.

II. THEORETICAL MODEL FOR PHASE DYNAMICS

In this section, we derive the equation of motion for the phase differences. Here, we describe the phase dynamics of the LJJ by neglecting the dissipation effect, for simplicity, but this effect is included later in the calucation of the fluxon trajectories in Sec. V. Also, we ngelect the boundary effect by considering a region away from the junction boundary in the x-direction (see Fig. 1), where the Josephson critical current density J_c^o in the absence of i-soliton is spatially not uniform.[28] We discuss the boundary effect of vanishing Josephson critical

current on the I-V curves in Sec. V.

We start with the following model Hamiltonian: $\hat{\mathcal{H}} = \sum_\ell \hat{\mathcal{H}}_{TB,\ell} + \hat{\mathcal{H}}_T$. Here the Hamiltonian $\hat{\mathcal{H}}_{TB,\ell}$ accounts for the two-gap superconductivity in the ℓ-th S layer, while the Hamiltonian $\hat{\mathcal{H}}_T$ accounts for electron tunneling between the two adjacent S layers. First, we consider these Hamiltonian condtibutions in the absence of electromagnetic fields. We write the two-gap Hamiltonian $\hat{\mathcal{H}}_{TB,\ell}$, as

$$\hat{\mathcal{H}}_{TB,\ell} = \int d\mathbf{r} \left(\sum_{i=s,d} \varepsilon^i c^{i\dagger}_{\sigma,\ell} c^i_{\sigma,\ell} + \hat{\mathcal{H}}^{pair}_\ell \right) \tag{1}$$

where ε^i describes the energy of electrons in the i-band ($i = s, d$) about the Fermi energy. For definiteness, we denote the two electronic bands involved in superconductivity as s and d bands. The pairing interaction between electrons in the ℓ-th S layer is described by the Hamiltonian $\hat{\mathcal{H}}^{pair}_\ell$ written as

$$\begin{aligned}\hat{\mathcal{H}}^{pair}_\ell = &-V_{ss} c^{s\dagger}_{\uparrow,\ell} c^{s\dagger}_{\downarrow,\ell} c^s_{\downarrow,\ell} c^s_{\uparrow,\ell} - V_{dd} c^{d\dagger}_{\uparrow,\ell} c^{d\dagger}_{\downarrow,\ell} c^d_{\downarrow,\ell} c^d_{\uparrow,\ell} \\ &-V_{sd} (c^{s\dagger}_{\uparrow,\ell} c^{s\dagger}_{\downarrow,\ell} c^d_{\downarrow,\ell} c^d_{\uparrow,\ell} + h.c.) \ , \end{aligned} \tag{2}$$

where $c^{i\dagger}_{\sigma,\ell}$ ($c^i_{\sigma,\ell}$) denotes the operator which creates (destroys) an electron with spin σ in the i-band, and V_{ij} denotes the strength of pairing interaction between electrons in the i and j bands. On the other hand, the Hamiltonian $\hat{\mathcal{H}}_T$ describes the electron tunneling between the two adjacent S layers that are separated by the insulator (I) layer. This Hamiltonian is given by

$$\hat{\mathcal{H}}_T = \sum_{i \neq j, \sigma} (T_{ij} c^{i\dagger}_{\sigma,1} c^j_{\sigma,2} + h.c.) \ , \tag{3}$$

where T_{ij} denotes the tunneling matrix element for an electron from the j to i band.

Following Leggett,[3] we consider the subspace spanned by the BCS type function and introduce pairing operators

$$\hat{\Psi}^i_\ell = c^{i\dagger}_{\uparrow,\ell} c^{i\dagger}_{\downarrow,\ell} \tag{4}$$

to account for the two (i.e., s and d) condensates. Using the eigenvalues of the pairing operator $\hat{\Psi}^i_\ell$, we rewrite the Hamiltonian $\hat{\mathcal{H}}_{TB,\ell}$ as

$$\begin{aligned}\hat{\mathcal{H}}_{TB,\ell} = &f^s_\ell(|\Psi^s_\ell|^2) + f^d_\ell(|\Psi^d_\ell|^2) - V_{ss}|\Psi^s_\ell|^2 - V_{dd}|\Psi^d_\ell|^2 \\ &-V_{sd}(\Psi^{s*}_\ell \Psi^d_\ell + \Psi^{d*}_\ell \Psi^s_\ell) \ , \end{aligned} \tag{5}$$

where $f^i_\ell(|\Psi^i_\ell|^2)$ corresponds to the kinetic energy of the electrons in the i-band. In the absence of contribution from the interband pairing (i.e., $V_{sd} = 0$), the electrons in the two bands (i.e., s and d) do not interact. The independent one-band gap equation for the parameter $\Delta^i = V_{ii}\Psi^i$ may be obtained by minimizing Eq. (5). We may account for the phase effects of the two condensates by writing the complex pesudo-order parameter Ψ^a_ℓ as

$$\Psi^i_\ell = \Psi^i_{o,\ell} e^{i\theta^i_\ell} \ . \tag{6}$$

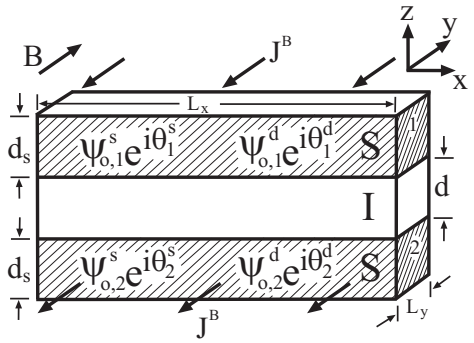

FIG. 1. A LJJ with two-gap superconductor represented by two pseudo-order parameters $\Psi^s_o \exp(i\theta^s)$ and $\Psi^d_o \exp(i\theta^d)$ is shown schematically. Here, L_x and L_y denote the dimensions in $x-$ and $y-$direction, respectively. J^B is the bias current density and B is the externally applied magnetic field. d_s and d denote the thickness of the superconductor (S) and insulator (I) layer, respectively.

In this respresentation, the interband pairing interaction term in Eq. (5) depends explicitly on the relative phase of the two condensates (i.e., s and d)

$$\chi_\ell = \theta^s_\ell - \theta^d_\ell \ . \tag{7}$$

The interband pairing contribution describes the Josephson effect within each S layer due to tunneling of the condensates between the two bands. Similarly, the conditions for the energy extremum yield the two coupled gap equations of the form

$$\Delta^i_\ell = \sum_j V_{ij} \Psi^j_\ell \ . \tag{8}$$

The coupled gap equations of Eq. (8) have two nontrivial solutions: $\chi_\ell = 0$ (i.e., $\theta^s_\ell = \theta^d_\ell$) and $\chi_\ell = \pi$ (i.e., $\theta^s_\ell = \theta^d_\ell + \pi$) corresponding to the S_{++} and S_{+-} symmetry, respectively. When $V_{sd} > 0$, $\chi_\ell = 0$ is the stable solution. On the other hand, when $V_{sd} < 0$, $\chi_\ell = \pi$ is the stable solution.

In addition to the phase-locked state, soft modes associated with fluctuations of χ_ℓ, representing a phase texture, may appear as a 2π-kink in χ_ℓ. These soft modes can modify the phase dynamics of LJJ. For example, these modes can manifest as resonances in the AC Josephson effect when the two electronic bands are out of equilibrium. Also, they may appear as 2π-kink representing an i-soliton.

We now investigate the effects of these soft modes by starting with the partition function $\mathcal{Z} = \mathrm{Tr} \exp[-\beta\mathcal{H}]$ for the LJJ with two-gap superconductors[29] in the presence of electromagnetic fields

$$\mathcal{Z} = \int \mathcal{D}[A^o, A] \mathcal{D}[\Psi^i_o] \mathcal{D}[\theta^i] e^{-\mathcal{S}[\Psi^i_o, \theta^i, A^o, A]} \ , \tag{9}$$

where $\beta = 1/T$ and T denotes temperature. Here, we set $\hbar = c = k_B = 1$ for convenience. The scalar and

vector potential in the ℓ-th layer are denoted by A^o_ℓ and $A_\ell = (A^x, A^y, A^z)_\ell$, respectively. The effective action $\mathcal{S} = \mathcal{S}_{gap} + \mathcal{S}_{field} - \mathrm{Tr}\,\hat{G}^{-1}$ is obtained by carrying out imaginary-time functional integral over the Grassmann fields $c^{i\dagger}_{\sigma,\ell}$ and $c^i_{\sigma,\ell}$. The contributions from the psudo-order parameter and electromagnetic fields are denoted by $\mathcal{S}_{gap}$ and $\mathcal{S}_{field}$, respectively. The expression for $\mathcal{S}_{gap}$ may be found in Appendix and $\mathcal{S}_{field}$ is included in the phase contribution, $\mathcal{S}_{phase}$, to the action below. Also, we do not write the explicit expression of the inverse Green function $\hat{G}^{-1}$ here but note that it is a 8x8 matrix which consists of a 4x4 matrix for each two-gap superconductor layer. We extract the superconducting phase degree of freedom by performing the unitary transformation for the Green function and follow the standard procedure[30] of retaining only the second-order tunneling processes arising from the Josephson effect. The usual imaginary-time functional integral approach[31] in this approximation allows us to obtain the phase contribution $\mathcal{S}_{phase}$ to the effective action $\mathcal{S}$, which includes the phase terms, in an external magnetic field B applied in the y-direction (see Fig. 1) as

$$\mathcal{S}_{phase} = \int_0^\beta d\tau \int dx\ \mathcal{L}_p\ . \tag{10}$$

The effective Lagrangian density $\mathcal{L}_p$ for the superconducting phases[31,32] is given by

$$\mathcal{L}_p = \frac{d_s}{8\pi\bar{e}^2}\sum_{i,\ell}\left[\frac{1}{\mu_i^2}\left(\frac{\partial\theta^i_\ell}{\partial\tau} + \bar{e}A^o_\ell\right)^2 - \frac{1}{\lambda_i^2}\left(\frac{\partial\theta^i_\ell}{\partial x} - \bar{e}A^x_\ell\right)^2\right] + \sum_{i,j}\frac{J^{ij}}{\bar{e}}\cos\varphi^{ij} + \sum_\ell\frac{J_{inter}}{\bar{e}}\cos\chi_\ell + \mathcal{L}_{EM}\ . \tag{11}$$

where $\bar{e} = 2e$, and d_s is the superconductor layer thickness. The phase difference of the superconduting order parameter in the magnetic field is $\varphi^{ij} = \theta^i_1 - \theta^j_2 - \bar{e}A^z_{1,2}$, where $A^z_{1,2} = \int_{\ell=1}^{\ell=2} A^z(z)dz$. The charge screening length $\mu_i = \sqrt{\lambda^2_{TF}/4\pi\epsilon_i}$ is a constant related to the Thomas-Fermi screening length $\lambda_{FT} = \sqrt{\pi a_o/4k_F}$, and the dielectric constant ϵ_i of the S layer. Here, a_o is the Bohr radius and k_F is the Fermi vector. The magnetic penetration depth of the S layer are denoted by $\lambda_i = \sqrt{m^o_i/4\pi n_i\bar{e}^2}$ where m^o_i is the mass of the i-band electron,

$$n_i = \sum_{\mathbf{k}}\frac{4\varepsilon^i_{\mathbf{k}}}{3E^i_{\mathbf{k}}}\left\{\tanh\frac{\bar{E}^i_{\mathbf{k}}}{2} + \bar{E}^i_{\mathbf{k}}f(E^i_{\mathbf{k}})[1 - f(E^i_{\mathbf{k}})]\right\}, \tag{12}$$

$E^i_{\mathbf{k}} = \sqrt{\varepsilon^2_{\mathbf{k}} + \Delta^i_{\mathbf{k}}}$, $\bar{E}^i_{\mathbf{k}} = \beta E^i_{\mathbf{k}}$, and $f(E)$ is the Fermi function. Here, we make a local approximation and consider μ and λ as constants.[30,31] The Josephson critical current J^{ij} betwen the electronic bands i and j in two adjacent S layers may be written[30,31] as

$$J^{ij} = -\frac{2\bar{e}}{d_s\beta}\int d\tau\sum_n e^{-i\omega_n\tau}\sum_{\mathbf{k},\mathbf{k}'}T^2_{ij}\frac{\Delta^i_{\mathbf{k}}\Delta^j_{\mathbf{k}'}}{E^i_{\mathbf{k}}E^j_{\mathbf{k}'}}\times \left\{\frac{E^i_{\mathbf{k}} - E^j_{\mathbf{k}'}}{(E^i_{\mathbf{k}} + E^j_{\mathbf{k}'})^2 + \omega_n^2}[f(E^i_{\mathbf{k}}) - f(E^j_{\mathbf{k}'})] + \frac{E^i_{\mathbf{k}} + E^j_{\mathbf{k}'}}{(E^i_{\mathbf{k}} + E^j_{\mathbf{k}'})^2 + \omega_n^2}[1 - f(E^i_{\mathbf{k}}) - f(E^j_{\mathbf{k}'})]\right\}, \tag{13}$$

where $\omega_n = 2n\pi/\beta$ with $n = 0, \pm1, \pm2, \cdots$ is the Matsubara frequency. The interband Josephson critical current $J_{inter} = 2\bar{e}V_{sd}\Psi^s_o\Psi^d_o/(V_{ss}V_{dd} - V^2_{sd})$ between the two bands within the same S layer does not represent charge transfer, as in J^{ij}. The Lagrangian density for the electromagnetic field $\mathcal{L}_{EM}$ in the insulator layer is given by

$$\mathcal{L}_{EM} = \frac{d}{8\pi}[\epsilon(E^z_{1,2})^2 - (B^y_{1,2})^2]\ , \tag{14}$$

where d is the I layer thickness, and ϵ is the dielectric constant. The electric and magnetic field between two adjacent S layers (i.e., $\ell = 1$ and $\ell = 2$) are defined as

$$E^z_{1,2} = -\frac{\partial A^z_{1,2}}{\partial t} - \frac{1}{d}(A^o_1 - A^o_2) \tag{15}$$

$$B^y_{1,2} = \frac{1}{d}(A^x_1 - A^x_2) - \frac{\partial A^z_{1,2}}{\partial x} \tag{16}$$

respectively.

We now derive the equations of motion for the phase difference φ^{ij} by following the usual approach of minimizing the action $\mathcal{S}_{phase}$ of Eq. (10). Here, noting that $\tau = -it$, we examine the phase dynamics of both φ^{ss} and φ^{dd} since we may write that $\varphi^{sd} = \theta^s_1 - \theta^d_2 + \bar{e}dA^z_{1,2} = \varphi^{ss} + \chi_2$ and $\varphi^{ds} = \theta^d_1 - \theta^s_2 + \bar{e}dA^z_{1,2} = \varphi^{ss} - \chi_1$. Using the Euler-Lagrange equation for the scalar and vector potentials (i.e., A^o_ℓ and A^z_ℓ), we obtain the following two coupled equations of motion for the phase differences φ^{ss} and φ^{dd}:

$$\eta^s_\mu\frac{\partial^2\varphi^{ss}}{\partial t^2} - \eta^s_\lambda\frac{\partial^2\varphi^{ss}}{\partial x^2} - \zeta_\mu\frac{\partial^2\varphi^{dd}}{\partial t^2} + \zeta_\lambda\frac{\partial^2\varphi^{dd}}{\partial x^2} + \frac{2J^{ss}}{\bar{e}}\sin\varphi^{ss} + \frac{J^{sd}}{\bar{e}}\left[\sin(\varphi^{ss} + \chi_2)\sin(\varphi^{ss} - \chi_1)\right] + \frac{J_{inter}}{\bar{e}}(\sin\chi_1 - \sin\chi_2) = 0\ , \tag{17}$$

and

$$\eta^d_\mu\frac{\partial^2\varphi^{dd}}{\partial t^2} - \eta^d_\lambda\frac{\partial^2\varphi^{dd}}{\partial x^2} - \zeta_\mu\frac{\partial^2\varphi^{ss}}{\partial t^2} + \zeta_\lambda\frac{\partial^2\varphi^{ss}}{\partial x^2} + \frac{2J^{ss}}{\bar{e}^2}\sin\varphi^{dd} + \frac{J^{sd}}{\bar{e}}\left[\sin(\varphi^{dd} - \chi_2)\sin(\varphi^{dd} + \chi_1)\right] - \frac{J_{inter}}{\bar{e}}(\sin\chi_1 - \sin\chi_2) = 0\ . \tag{18}$$

The coeffiecients in the above two equations of motion (for φ^{ss} and φ^{dd}) are

$$\eta^i_\xi = \frac{d_s}{4\pi\bar{e}^2\xi^2_i}\left(1 - \frac{d_s d}{4\pi\xi^2_i\kappa_\xi}\right) \tag{19}$$

and

$$\zeta_\xi = \left(\frac{d_s}{4\pi\bar{e}\xi_s\xi_d}\right)^2\frac{d}{\kappa_\xi}, \tag{20}$$

where

$$\kappa_\xi = \frac{d_s d}{4\pi}\left(\frac{1}{\xi_s^2}+\frac{1}{\xi_d^2}\right)+\kappa_\xi^o \ . \tag{21}$$

Here, ξ_i denotes either the screening length (μ_i) or the magnetic penetration depth (λ_i) of the i-band, $\kappa_\mu^o=\epsilon/2\pi$ and $\kappa_\lambda^o=1/2\pi$.

By noting that the phase difference φ^{sd} may be written as either $\varphi^{sd}=\varphi^{ss}+\chi_2$ or $\varphi^{sd}=\varphi^{dd}+\chi_1$, we may see straightforwardly that the phase dynamics for both φ^{dd} and φ^{ss} are closely related through the soft modes χ_1 and χ_2 in the two adjacent S layers. We simplify the equation of motion for φ^{ss} by writing that $\varphi^{dd}=\varphi^{ss}-\chi_1+\chi_2$. This substitution yields a familiar form of the equation of motion for both φ^{ss} and φ^{dd}. Here, we focus on the phase dynamics of φ^{ss} given by

$$\frac{d_s}{4\pi\bar{e}^2}\left(\frac{\kappa_\mu^o}{\mu_s^2\kappa_\mu}\frac{\partial^2\varphi^{ss}}{\partial t^2}-\frac{\kappa_\lambda^o}{\lambda_s^2\kappa_\lambda}\frac{\partial^2\varphi^{ss}}{\partial x^2}\right)+\frac{2J^{ss}}{\bar{e}}\sin\varphi^{ss} + \frac{J^{sd}}{\bar{e}}\left[\sin(\varphi^{ss}+\chi_2)+\sin(\varphi^{ss}-\chi_1)\right] \tag{22}$$

$$+\sum_{\ell=1}^{2}(-1)^{\ell+1}\left[\zeta_\mu\frac{\partial^2\chi_\ell}{\partial t^2}-\zeta_\lambda\frac{\partial^2\chi_\ell}{\partial x^2}+\frac{J_{inter}}{\bar{e}}\sin\chi_\ell\right]=0 \ .$$

As indicated by Eq. (22), the phase dynamics of φ^{ss} depend strongly on the relative phases (i.e., χ_1 and χ_2) of the two condensates. As the phase χ_ℓ depends only on the interband Josephson effect, it is not influenced by the dynamics of the phase difference φ^{ss} across the junction. Hence we may separate the phase dynamics decribed by Eq. (22) into two separate equations. Assuming that $\chi_1=\chi_2=\chi$, we write these equations as

$$\frac{\partial^2\varphi^{ss}}{\partial\bar{x}^2}-\frac{\partial^2\varphi^{ss}}{\partial\bar{t}^2}-\left(1+\frac{J^{sd}}{J^{ss}}\cos\chi\right)\sin\varphi^{ss}=0 \ , \tag{23}$$

$$\frac{\partial^2\chi}{\partial\tilde{x}^2}-\frac{\partial^2\chi}{\partial\tilde{t}^2}-\sin\chi=0 \ , \tag{24}$$

where $(\bar{t},\bar{x})$ and $(\tilde{t},\tilde{x})$ are the dimensionless coordinates for the phases φ^{ss}, and χ, respectively. Here, it is note that, we may assume that $\varphi^{ss}=\varphi^{dd}$ when $\chi_1=\chi_2$. This suggests that the two tunneling channels (i.e., $\varphi^{ss}=\varphi^{dd}$) become equivalent.

III. INTERBAND JOSEPHSON EFFECT

In this section, we derive the equation of motion for the interband phase difference χ of Eq. (24) from the two-band Hamiltonian $\hat{\mathcal{H}}_{TB,\ell}$ of Eq. (1). It is noted that this Hamiltonian accounts for excitation of an i-soliton due to the interband Josephson effect. By following Leggett,[3] we write the two-band Hamiltonian in the $\mathbf{k}$-space representation as

$$\hat{\mathcal{H}}_{TB,\ell}=\sum_{i=s,d}\hat{\mathcal{H}}^i_{OB,\ell}-\hat{E}_o+\hat{\mathcal{H}}^{pair}_{inter,\ell}+E_{ng}+\hat{\mathcal{H}}^{ci}_\ell \ , \tag{25}$$

where the Hamiltonian $\hat{\mathcal{H}}^i_{OB,\ell}$ for the electronic band i is given by

$$\hat{\mathcal{H}}^i_{OB,\ell}=\sum_{\mathbf{k},\sigma,\ell}\varepsilon^i_{\mathbf{k}}c^{i\dagger}_{\mathbf{k}\sigma,\ell}c^i_{\mathbf{k}\sigma,\ell}-V_{ii}\sum_{\mathbf{k},\mathbf{k}'}c^{i\dagger}_{\mathbf{k}\uparrow,\ell}c^{i\dagger}_{-\mathbf{k}\downarrow,\ell}c^i_{-\mathbf{k}'\downarrow,\ell}c^i_{\mathbf{k}'\uparrow,\ell}. \tag{26}$$

Here, we introduce $\hat{E}_o$ so that the ground-state energy of $\sum_i\hat{\mathcal{H}}^i_{OB,\ell}-\hat{E}_o$ in the normal state vanishes for an arbitrary value of N_s and N_d, which denote the number of electrons in the s and d-band, respectively. The interband pairing interaction between the electrons in s and d band is decribed by the Hamiltonian $\hat{\mathcal{H}}^{pair}_{inter,\ell}$ which may be written as

$$\hat{\mathcal{H}}^{pair}_{inter,\ell}=-V_{sd}\sum_{\mathbf{k},\mathbf{k}',i\neq j}c^{i\dagger}_{\mathbf{k}\uparrow,\ell}c^{i\dagger}_{-\mathbf{k}\downarrow,\ell}c^j_{-\mathbf{k}'\downarrow,\ell}c^j_{\mathbf{k}'\uparrow,\ell} \ . \tag{27}$$

The term E_{ng} denotes the ground-state energy of the system in the normal state. This energy E_{ng} is fixed by the total number of electrons $N=N_s+N_d$ in the system. The Hamiltonian $\hat{\mathcal{H}}^{ci}_\ell$ accounts for the effects of charge fluctuations from the equilibrium state. These charge fluctuations may arise from either the boundary conditions, various residual scattering processes, or the chemical potential fluctuations and lead to the charge imbalance between the s and d-band. The Hamiltonian $\hat{\mathcal{H}}^{ci}_\ell$ may be approximated[3] as

$$\hat{\mathcal{H}}^{ci}_\ell=\gamma_o[(\hat{N}_s-\hat{N}^o_s)-(\hat{N}_d-\hat{N}^o_d)]^2_\ell=\gamma(\delta\hat{N}_\ell)^2 \tag{28}$$

when the deviation from the equilibrium is small. Here, $\gamma_o=(\rho_s^{-1}+\rho_d^{-1})/8$, $\rho_i=m_i^o k_F/\pi^2$ denotes the density of states for the i-band electrons at the Fermi surface, and $\hat{N}^o_i$ denotes the number operator for the i-band electrons in the equilibrium state.

To assess the dynamics of relative phase χ_ℓ due to the interband Josephson effect, we rewrite the two-band Hamiltonain $\hat{\mathcal{H}}_{TB,\ell}$ in terms of the familiar Ginzberg-Landau (GL) free energy. (See Appendix for a detail discussion on the derivation of GL free energy for the two-gap superconuctors.) Here, we note that the temperature range is restricted to $(T_c-T)/T_c\ll 1$, where T_c is the superconducting transition temperature. Also, we considered the zero field limit here since the interband phase fluctustions do not carry magnetic flux. In the absence of magnetic field, we may write the one-band Hamiltonian $\hat{\mathcal{H}}^i_{OB,\ell}$ in the form of the GL free energy[33] $\mathcal{G}^i_{OB,\ell}$ as a function of pseudo-order parameter Φ^i_ℓ (i.e., $\sum_i\hat{\mathcal{H}}^i_{OB,\ell}-E_o\rightarrow\sum_i\mathcal{G}^i_{OB,\ell}$). Here, Φ^i_ℓ is the auxilary field representing an electron pair. For one spatial dimensional case, we may write $\mathcal{G}^i_{OB,\ell}$ as

$$\mathcal{G}^i_{OB,\ell}=a_i^{GL}|\Phi^i_\ell|^2+\frac{b_i^{GL}}{2}|\Phi^i_\ell|^4+\frac{1}{2m_i^*}\left|\frac{d\Phi^i_\ell}{dx}\right|^2 \ , \tag{29}$$

where a_i^{GL} and b_i^{GL} are the coefficients of the GL free energy and m_i^* is the effective mass of the electron in the i-band. (See Appendix.) When the order parameter Φ^i_ℓ is written in terms of the modulus-phase variables

(i.e., $\Phi^i_\ell = |\Phi^i_\ell| \exp(i\theta^i_\ell)$), the interband pairing interaction $\hat{\mathcal{H}}^{pair}_{inter,\ell}$ yields the contribution

$$\mathcal{G}^{pair}_{inter,\ell} = -\frac{2g_{sd}}{g_s g_d}|\Phi^s_\ell||\Phi^d_\ell|\cos(\theta^s_\ell - \theta^d_\ell)\ , \qquad (30)$$

where $g_i = (V_{ss}V_{dd} - V^2_{sd})/V_{ii}$ and $g_{sd} = V_{sd}(V_{ss}V_{dd} - V^2_{sd})/(V_{ss}V_{dd})$. Here, we assumed that the intraband interaction is much larger than the interband interaction (i.e., $V_{ij} \ll V_{ii}$). With this assumption, we may approximate that $|\Phi^a_\ell| \sim \sqrt{N_a}$, which specifies that the intraband interaction is independent of the coordinates (i.e., $d|\Phi^a_\ell|/dx \approx 0$). The charge-imbalance contribution $\hat{\mathcal{H}}^{ci}_\ell$ in Eq. (25) may be expressed in a familiar form by using the number-phase uncertainty relationship of

$$[\delta\hat{N}_\ell, \hat{\theta}^s_{\ell'} - \hat{\theta}^d_{\ell'}] = -4i\delta_{\ell\ell'}, \qquad (31)$$

where $\delta_{\ell\ell'}$ is the kronecker delta. Noting that the Heisenberg equation of motion for the phase difference $\hat{\chi}_\ell = \hat{\theta}^s_\ell - \hat{\theta}^d_\ell$ is given by

$$\frac{d\hat{\chi}_\ell}{dt} = i[\hat{\chi}_\ell, \hat{\mathcal{H}}_{TB,\ell}], \qquad (32)$$

we may write

$$\mathcal{G}^{ci}_\ell = \frac{1}{64\gamma_o}\left(\frac{d\chi_\ell}{dt}\right)^2\ . \qquad (33)$$

Combining the result of Eqs. (29), (30) and (33), we may write the Gibbs free energy density $\bar{\mathcal{G}}_{TB} = \sum_i(\mathcal{G}^i_{OB} - \mathcal{G}^i_{ng})$ for the two-gap superconductor in the superconducting state as

$$\bar{\mathcal{G}}_{TB,\ell} = \sum_i\left(a^{GL}_i|\Phi^i_\ell| + \frac{b^{GL}_i}{2}|\Phi^i_\ell|^4 + \frac{|\Phi^i_\ell|^2}{2m^*_i}\left|\frac{d\theta^i_\ell}{dx}\right|\right) + \frac{1}{64\gamma_o}\left(\frac{d\chi_\ell}{dt}\right)^2 - \frac{2g_{sd}}{g_s g_d}|\Phi^s_\ell||\Phi^d_\ell|\cos\chi_\ell\ . \qquad (34)$$

Here, we assumed that the effects of external fields are weak inside each S layer and, thereby, their contributions in $\bar{\mathcal{G}}_{TB,\ell}$ are neglected.

We now use the Gibbs free energy of Eq. (34) and obtain the equation of motion for χ_ℓ. By noting that there is no supercurrent J_ℓ flowing anywhere inside the bulk superconductor, we write that

$$J_\ell = \sum_i \frac{|\Phi^i_\ell|}{m^*_i}\frac{d\theta^i_\ell}{dx} = 0. \qquad (35)$$

From the condition that $J_\ell = 0$, it is straightforward to obtain that

$$\theta^d_\ell = -\frac{m^*_d|\Phi^s_\ell|}{m^*_s|\Phi^d_\ell|}\theta^s_\ell + \delta_o\pi. \qquad (36)$$

Here, $\delta_o = 0$ for $J_{inter} < 0$ (S_{+-} symmetry) and $\delta_o = 1$ for $J_{inter} > 0$ (S_{++} symmetry). We minimize the Gibbs free energy density with respect to the phase variation (i.e., $d\bar{\mathcal{G}}_{TB,\ell}/d\chi_\ell = 0$) and obtain the equation of motion for χ_ℓ as

$$\frac{d^2\chi_\ell}{d\bar{x}^2} - \frac{d^2\chi_\ell}{d\bar{t}^2} - \sin\chi_\ell = 0\ , \qquad (37)$$

where the dimensionless cooridnates $(\bar{x},\ \bar{t})$ are $\bar{x} = [4g_{sd}(m^*_s|\Phi^d|^2 + m^*_d|\Phi^s|^2)/g_s g_d|\Phi^s||\Phi^d|]^{1/2}x$ and $\bar{t} = t/(128\gamma_o g_{sd}|\Phi^s||\Phi^d|/g_s g_d)^{1/2}$. It is straightfoward to see that Eq. (37) may yield a number of soliton solutions, but, for simplicity, we consider a single-soliton solution of

$$\chi_\ell(\bar{x},\bar{t}) = 4\tan^{-1}\left[\exp\left(\pm\frac{\bar{x} - \upsilon_o\bar{t}}{\sqrt{1-\upsilon^2_o}}\right)\right], \qquad (38)$$

which is a kink-solution, known as the i-soliton. Here υ_o is the speed of i-soliton. The kink-solution of Eq. (38) is identical to the functional form of the unperturbed fluxon solution.[24] However, the property of i-soliton differs from that of the fluxon. Unlike fluxon, an i-soliton does not carry a quantum of magnetic flux and cannot be driven by the Lorentz force due to the the bias current J^B as shown in Fig. 1.

The equation of motion for χ_ℓ and its solution of Eq. (38) indicates that the perturbation effects in the two-gap superconductor may lead the relative phase χ_ℓ to fluctuate from the phase-locked state of χ_ℓ. These phase fluctuations, in turn, yield collective excitations, but they modify neither the ground state nor the one-particle excitation spectrum. However, if large phase fluctuations representing a 2π-phase texture can be stablized, then the one-particle excitation spectrum may become modified.

IV. EFFECTS OF i-SOLITION ON PHASE DYNAMICS

We now examine the effects of large fluctuations in the relative phase of the s and d condensates on the fluxon dynamics. When the amplitude of these phase fluctuations grows to the nonlinear region and becomes stablized as suggested by Tanaka,[17] excitation of an i-soliton can change the amplitude of critical current density. The modulation of critical current between two adjacent S layers may be considered as an effective potential for a fluxon. The effects of an i-soliton excitation on the phase dynamics of the LJJ may be described by Eq. (23). We may simplify Eq. (23) by substituting Eq. (38). The equation of motion for the fluxon which accounts for the interband Josephson effect in each S layer is given as

$$\frac{\partial^2\varphi}{\partial\bar{x}^2} - \frac{\partial^2\varphi}{\partial\bar{t}^2} - \frac{J_c}{J^o_c}\sin\varphi = 0, \qquad (39)$$

where $\varphi = \varphi^{ss}$, $J_c/J^o_c = 1 + (J^{sd}/J^{ss})[1 - 2\mathrm{sech}^2(\alpha_o\bar{\mathrm{x}} - \beta_o\bar{\mathrm{t}})]$ and J^o_c is the critical current in the absence of

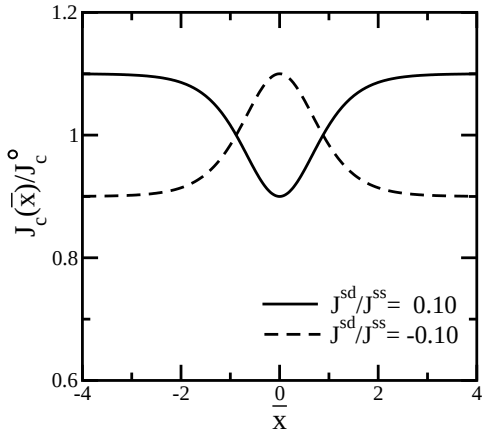

FIG. 2. The amplitude modulation of the Josephson current density $J_c(\bar{x})/J_c^o$ due to excitation of static i-soliton representing 2π-phase texture with its center located at $x = 0$ is illustrated for the interband Josephson current density of $J^{sd}/J^{ss} = 0.10$ (solid line) and -0.10 (dashed line). Here, J_c^o is the critical current density of the homogenous LJJ in the absence of the interband Josephson effect.

the interband Josephson effect (i.e., $J^{sd} = 0$). Here $\alpha_o = [J^{sd}\lambda_d^2/(1-\upsilon_o^2)J^{ss}d_s d]^{1/2}$ and $\beta_o = \upsilon_o[J^{sd}\mu_d^2\epsilon/(1-\upsilon_o^2)J^{ss}d_s d]^{1/2}$. Equation (39) indicates that a i-soliton, representing a moving 2π-phase texture of Eq. (38), leads to both spatial and temporal dependent modulation of the critical current.

The effects of spatial and temporal variation of J_c/J_c^o on the fluxon depend on the shape of this modulation. In Fig. 2, we neglect the temporal modulation and plot the amplitude of the critical current (J_c/J_c^o) versus the dimensionless spatial coordinate $\bar{x}$ for J^{sd}/J_c^o=0.1 (solid line) and -0.1 (dashed line) to illustrate the effects of a single i-soliton excitation in the S_{++} and S_{+-} symmetry superconductor, respectively. Here, we set $\alpha_o = 1$ for definiteness. The curves show that the shape of critical current modulation depends on the symmetry of order parameter (i.e., S_{++} versus S_{+-}). However, as we discuss in Sec. V, when $J^{sd}/J^{ss} \ll 1$, the symmetry of the order parameter does not affect the fluxon motion significantly.

The critical current modulation induced by the interband Josephson effect has two main effects. First, the shape of fluxon may become deformed. However, for a small modulation considered in the present work, this effect is negligible. Second, the speed of fluxon becomes modified since the critical current modulation behaves as an effective potential. In the region of critical current modulation, the fluxon speed may become significantly changed from a uniform value. These changes imply that the EM waves can be emitted by a moving fluxon as it decelerates.

We use the perturbation method to examine the effects of critical current modulation on the emission of EM waves. To obtain physical insight, we carry out the calculation in the rest frame of the fluxon (i.e., a reference frame which is moving with the speed of the unperturbed fluxon) as described[34] by Fogel and coworkers. To this end, we perform the Lorentz transformation of

$$\bar{t}' = \frac{\bar{t} - \upsilon\bar{x}}{\sqrt{1-\upsilon^2}} \quad \text{and} \quad \bar{x}' = \frac{\bar{x} - \upsilon\bar{t}}{\sqrt{1-\upsilon^2}} \ , \tag{40}$$

where υ is the speed of the unperturbed fluxon. With this transformation, we rewrite the sine-Gordon equation of Eq. (39) as

$$\frac{\partial^2\varphi}{\partial\bar{x}'^2} - \frac{\partial^2\varphi}{\partial\bar{t}'^2} - \frac{\bar{J}_c}{J_c^o}\sin\varphi = 0 \ , \tag{41}$$

where $\bar{J}_c/J_c^o = 1 + (J^{sd}/J^{ss})[1 - 2\mathrm{sech}^2(\alpha_o'\bar{x}' + \beta_o'\bar{t}')]$, $\alpha_o' = (\alpha_o - \beta_o\upsilon)/\sqrt{1-\upsilon^2}$ and $\beta_o' = (\alpha_o\upsilon - \beta_o)/\sqrt{1-\upsilon^2}$.

By considering the case of weak interband Josephson effect (i.e. $J^{sd}/J^{ss} \ll 1$), we assume that a solution to Eq. (41) may be written as

$$\varphi(x,t) \approx \varphi_o(x) + \frac{J^{sd}}{J^{ss}}\varphi_1(x,t) \ . \tag{42}$$

Here, for convenience, we make the following changes in the notation: $(\bar{x}', \bar{t}') \to (x,t)$. A solution to the unperturbed sine-Gordon equation of

$$\frac{\partial^2\varphi_o}{\partial x^2} - \frac{\partial^2\varphi_o}{\partial t^2} - \sin\varphi_o = 0 \tag{43}$$

is given by $\varphi_o(x) = 4\tan^{-1}[\exp(x)]$. Following Fogel et al.,[34] we may write the correction term φ_1 due to the critical current modulation in the most appropriate basis by separating the spatial and temporal dependence as

$$\varphi_1(x,t) = f(x)e^{-i\omega t} \ . \tag{44}$$

The separation of variables for the perturbative contribution φ_1 in the rest frame of the fluxon (i.e., $\upsilon = 0$) leads to the eigenvalue equation for $f(x)$ as

$$\left[-\frac{d^2}{dx^2} + (1 - 2\mathrm{sech}^2 x)\right] f(x) = \omega^2 f(x) \ . \tag{45}$$

The eigenvalue problem of Eq. (45) yields one bound state with $\omega = \omega_b = 0$ and a continuum of scattering states with $\omega^2 = \omega_\kappa^2 = 1 + \kappa^2$. The corresponding normalized eigenfunctions are

$$f(x) = \begin{cases} f_b(x) = 2\mathrm{sech}x \ , & \text{with } \omega = \omega_b \\ f(\kappa, x) = \frac{\kappa + i\tanh x}{\sqrt{2\pi}\omega_\kappa} e^{i\kappa x}, & \text{with } \omega = \omega_\kappa \end{cases} \tag{46}$$

Here we use the subscripts b and κ to denote the bound state and continuum of scattering state κ, respectively. The bound state $f_b(x)$ is associated with the Goldstone translation mode of the fluxon, while the continuum eigenfunctions $f(\kappa, x)$ represent the radiation modes. The eigenfunction of Eq. (46) indicates that the first order correction $\varphi_1(x,t)$ due to the critical current modulation may be separated into two parts as

$$\varphi_1(x,t) = \varphi_{trans}(x,t) + \varphi_{rad}(x,t) \ . \tag{47}$$

Here, φ_{trans} and φ_{rad} represent the bound state and continuum eigenstate contribution, respectively.

The bound state contribution $\varphi_{trans}(x,t)$ may be written as

$$\varphi_{trans}(x,t) = \frac{1}{8}\phi_b(t) f_b(x) \ . \tag{48}$$

The amplitude $\phi_b(t)$ of the bound state is determined straightforwardly from the equation of

$$\frac{d^2\phi_b(t)}{dt^2} = 4\int_{-\infty}^{\infty} dx(1-2\mathrm{sech}^2\xi_o)\frac{\sinh x}{\mathrm{sech}^2 x} \tag{49}$$

where $\xi_o = \alpha_o' x + \beta_o' t$. The solution to Eq. (49) may be obtained as

$$\phi_b(t) = -\frac{8\alpha_o'}{\beta_o'^2}\left(1 - \int_{-\infty}^{\infty} dx \frac{\mathrm{sech}^2 x}{e^{2\beta_o' t}e^{2\alpha_o' x}+1}\right). \tag{50}$$

We note that $\phi_b(t)$ may be used to evaluate the translation mode contribution $\varphi_{trans}(x,t)$. This contribution has no effects on the motion of the fluxon center.

The continuum eigenstate contribution, representing the radiation modes, is given by

$$\varphi_{rad}(x,t) = \int_{-\infty}^{\infty} d\kappa \ \phi(\kappa,t) f(\kappa,x). \tag{51}$$

The amplitude $\phi(\kappa,t)$ is determined from

$$\frac{d^2\phi(\kappa,t)}{dt^2} + (1+\kappa^2)\phi(\kappa,t) = \mathcal{Q}(\kappa,t) \ , \tag{52}$$

where

$$\mathcal{Q}(\kappa,t) = 2\int_{-\infty}^{\infty} dx f^*(\kappa,x)(1-2\mathrm{sech}^2\xi_o)\frac{\sinh x}{\cosh^2 x}. \tag{53}$$

In obtaining Eq. (52), we used the orthonormality condition for the eigenfunctions (i.e., $\int dx f^*(\kappa',x) f(\kappa,x) = \delta(\kappa-\kappa')$). The contribution to the radiation mode of φ_1 may be estimated by solving Eq. (52). For a single modulation of the critical current density as shown in Fig. 2, we may obtain a solution to Eq. (52) more easily by using the relation

$$\mathrm{sech}^2\xi_o = \int_{-\infty}^{\infty}\frac{dk}{2\pi}\frac{\pi k}{\sinh\frac{\pi k}{2}}e^{ik\xi_o} \tag{54}$$

which is the Fourier representation of the critical current variation. Using this substitution, we rewrite $\mathcal{Q}(\kappa,t)$ by integrating the right hand side of Eq. (53) over x and obtain

$$\mathcal{Q}(\kappa,t) = \frac{-i\pi}{\sqrt{2\pi(1+\kappa^2)}}\Bigg\{(1+\kappa^2)\mathrm{sech}\frac{\kappa\pi}{2} - \int_{-\infty}^{\infty} dk \frac{\mathrm{sech}\frac{\pi k\eta_\kappa}{2}}{2\sinh\frac{\pi k}{2}}[1+\kappa^2-(k\alpha)^2]ke^{ik\beta_o' t}\Bigg\}, \tag{55}$$

where $\eta_\kappa = \alpha_o' - (\kappa/k)$. The solution $\phi(\kappa,t)$ may be written as

$$\phi(\kappa,t) = \int_{-\infty}^{\infty}\frac{d\omega}{2\pi}\frac{\mathcal{Q}(\kappa,\omega)}{(1+\kappa^2)-\omega^2}e^{i\omega t}. \tag{56}$$

where $\mathcal{Q}(\kappa,\omega) = \int dt' \mathcal{Q}(\kappa,t')\exp(-i\omega t')$. It is straightforward to evaluate the integration over t' and ω, and write the solution $\phi(\kappa,t)$ as

$$\phi(\kappa,t) = \frac{-i\pi}{\sqrt{2\pi(1+\kappa^2)}}\Bigg[\mathrm{sech}\frac{\kappa\pi}{2} - \int_{-\infty}^{\infty} dk \frac{\mathrm{sech}\frac{\pi k\eta_\kappa}{2}}{\sinh\frac{\pi k}{2}}\frac{1+\kappa^2-(k\alpha_o')^2}{1+\kappa^2-(k\beta_o')^2}ke^{ik\beta_o' t}\Bigg] \tag{57}$$

However, as indicated in Eq. (51), we need to integrate over the continuum variable κ to compute $\varphi_{rad}(x,t)$. This may be evaluated by using the contour integration method. The location of the poles for the contour integral is shown schematically in Fig. 3. The radiation contribution $\varphi_{rad}(x,t)$ of Eq. (51) indicates that all poles are simple, and the residue of each pole may be evaluated separately. The location of the poles are the following: $z_o = +i$, $z_1 = +i\sqrt{1-(k\beta_o')^2}$, $z_n^o = +i(2n+1)$, and $z_n^{\pm} = \pm k\alpha_o' + i(2n+1)$, where $n = 0, 1, 2, \cdots$. The residues of the pole structure shown in Fig. 3 yield two types of contribution: i) exponentially localized contribution around the fluxon center and ii) linear traveling wave contribution. Hence, we may decompose the radiation mode φ_{rad} into the exponentially localized (φ_{rad}^{exp}) and traveling wave (φ_{rad}^{wave}) contributions: $\varphi_{rad} = \varphi_{rad}^{exp} + \varphi_{rad}^{wave}$. We note that the exponentially localized contribution φ_{rad}^{exp} does not produce a true radiative correction. Only the traveling wave φ_{rad}^{wave} gives rise to a true radiative contribution.

We now focus on the poles that give rise to the traveling wave contribution to the radiation correction. As indicated by the Fourier components of the critical current modulation decribed by the $(1-2\mathrm{sech}^2\xi_o)$ factor in Eq. (53), the condition for traveling wave radiative contribution depends on k. For fixed $k < (1/\beta_o')$, the pole at z_1 lies on the imaginary axis as shown in Fig. 3. However, as the fluxon speed υ increases, the pole z_1 moves down the imaginary axis. At the critical value $\upsilon = \upsilon_{th}$, the pole z_1 lies at the complex plane and it becomes real when $\upsilon > \upsilon_{th}$. The changes in the radiation contribution in Eq. (51) from this pole may be easily identified by the contour integration since it is not exponentially localized around the fluxon center but oscillates with x. The oscillatory contribution only arises when $\upsilon > \upsilon_{th}$. This leads to the radiative contribution of

$$\varphi_{rad}^{wave}(x,t) = -\int_{\frac{1}{\beta_o'}}^{\infty}\frac{dk}{2\eta}\frac{\pi k}{\sinh\frac{\pi k}{2}}(\eta + i\tanh x)\times \left(1-\frac{\alpha_o'^2}{\beta_o'^2}\right)\left[\frac{e^{ik(\beta_o' t+\eta x)}}{\cosh\frac{\pi k\eta_-}{2}} + \frac{e^{-ik(\beta_o' t-\eta x)}}{\cosh\frac{\pi k\eta_+}{2}}\right] \ , \tag{58}$$

where $\eta = \sqrt{(k\beta_o')^2 - 1}$, and $\eta_\pm = \alpha_o' \mp (\eta/k)$. Equation (58) indicates that, for a fixed k, this radiation correction

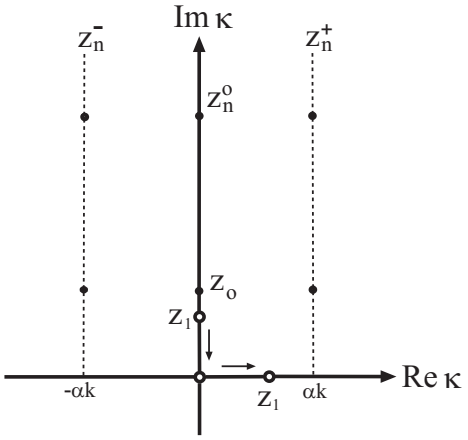

FIG. 3. The pole structure for the radiation contribution of Eq. (51) to $\varphi_1(\kappa, t)$ for a fixed k is shown schematically. The solid circles represent the poles yielding the exponentially localized contribution. The open circles represent the changes in the location of z_1 as the fluxon velocity v changes from $v < v_{th}$ (on the imaginary axis) to $v > v_{th}$ (on the real axis). The shift direction for the pole z_1 is indicated by the arrows.

is the superposition of two linear traveling waves with different amplitudes. The two waves travel in opposite directions. The threshold velocity v_{th} for the fluxon is given by

$$v_{th} = v_o \left(\frac{\mu_d^2 \epsilon}{\lambda_d^2} \right)^{1/2} . \tag{59}$$

The dependence of v_{th} on the i-soliton velocity v_o indicates that, for the case of static spatial variation of the phase (i.e., $v_o = 0$), EM radiation may be emitted by the fluxon whenever it passes through a region where the critical current is affected by the interband Josephson effect. Hence, when an array of static i-solitons are excited to yield a sptially periodic modulation of the critical current density, the threshold velocity v_{th} becomes finite. This radiative threshold is similar to that found in earlier studies.[25–27]

V. CURRENT-VOLTAGE CHARACTERISTICS

Emission of EM radiation by a moving fluxon, indicated by the linear traveling wave contribution to the raditive correction in $\varphi_1(x, t)$ as discussed in Sec. IV, reflects the changes in the fluxon dynamics. We now examine the effects of a single i-soliton excitation on fluxon dynamics by considering a static phase texture described by Eq. (39) with $v_o = 0$ (i.e., $\beta_o = 0$). Here, we include the perturbative effects of bias current and dissipation to examine a realistic tunnel junction. The bias current J^B acts as a driving force for the fluxon, while the two dissipation terms, $\Gamma_1(\partial\varphi/\partial\bar{t})$ and $\Gamma_2(\partial^3\varphi/\partial\bar{t}\partial^2\bar{x})$, account for the interaction between the fluxon and dissipative environment. Using the perturbed sine-Gordon equation with the critical current density modulation, we determine the fluxon trajectories and estimate the effects of the bias current and dissipation (Γ_1 and Γ_2). These perturbation contributions as well as the interband Josephson effect can modify the current-voltage curve. We start with the perturbed sine-Gordon equation of

$$\frac{\partial^2\varphi}{\partial\bar{x}^2} - \frac{\partial^2\varphi}{\partial\bar{t}^2} - \sin\varphi = \mathcal{F}(\varphi, \bar{x}, \bar{t}) \tag{60}$$

where the perturbation term $\mathcal{F}(\varphi, \bar{x}, \bar{t})$ is given by

$$\mathcal{F}(\varphi, \bar{x}, \bar{t}) = \frac{J^{sd}}{J^{ss}}[1 - \mathrm{sech}^2(\alpha_o\bar{x})]\sin\varphi - \frac{J^B}{J_c^o} + \Gamma_1\frac{\partial\varphi}{\partial\bar{t}} + \Gamma_2\frac{\partial^3\varphi}{\partial\bar{t}\partial^2\bar{x}} . \tag{61}$$

Here, we assume that each perturbation term in $\mathcal{F}$ is small and does not change the shape of the fluxon in the leading order. The main effect of the first term of $\mathcal{F}$ in Eq. (61) is to provide a potential for a moving unperturbed fluxon of

$$\varphi_o(\bar{x}, \bar{t}) = 4\tan^{-1}(e^{\zeta}) , \tag{62}$$

where

$$\zeta(\bar{x}, \bar{t}) = \pm\frac{\bar{x} - \int_0^{\bar{t}} v(t')dt' - \bar{x}_o(\bar{t})}{\sqrt{1 - v^2(\bar{t})}} . \tag{63}$$

Here, the fluxon speed $v(\bar{t})$ accounts for the time dependence induced by the critical current modulation. We now examine the trajectories of the fluxon in a LJJ, and the effects of a i-soliton excitation on the I-V curve in the low-voltage regime.

By following McLaughlin and Scott,[24] we examine the fluxon trajectories by computing the fluxon speed and the corresponding position. For this purpose, we assume that the fluxon approaches the region of a large stable variation of phase difference (i.e., 2π-phase texture) between the s and d condensates from $\bar{x} = -\infty$ with increasing $\bar{t}$. We write Eq. (60) as two first order differential equations describing the velocity (v) and the position ($\bar{x}_o$) of the fluxon, respectively, as

$$\frac{dv}{d\bar{t}} = \mp\frac{1 - v^2}{4}\int_{-\infty}^{\infty} d\bar{x}\ \mathcal{F}(\varphi_o, \bar{x}, \bar{t})\ \mathrm{sech}\zeta , \tag{64}$$

$$\frac{d\bar{x}_o}{d\bar{t}} = -\frac{v}{4}\sqrt{1 - v^2}\int_{-\infty}^{\infty} d\bar{x}\ \mathcal{F}(\varphi_o, \bar{x}, \bar{t})\ \zeta\mathrm{sech}\zeta, \tag{65}$$

where $\zeta = \zeta(\bar{x}, \bar{t})$ is defined in Eq. (63). The perturbation term $\mathcal{F}$ modifies the speed v of the unperturbed wave form of Eq. (62) to depend on time $\bar{t}$. By performing the integration, we rewrite Eqs. (64) and (65), which respectively account for the fluxon speed v and position X, as

$$\frac{dv}{d\bar{t}} = \pm\frac{\pi}{4}\frac{J^B}{J_c^o}(1 - v^2)^{\frac{3}{2}} - \Gamma_1 v(1 - v^2) - \frac{1}{3}\Gamma_2 v + (1 - v^2)^{\frac{3}{2}}\frac{J^{sd}}{J^{ss}}\int_0^{\infty} dy\Upsilon_+\frac{\sinh y}{\cosh^3 y} \tag{66}$$

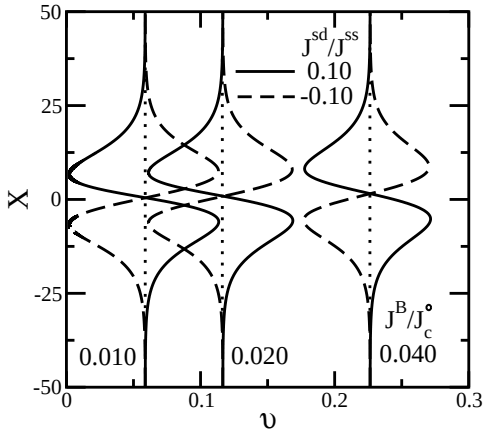

FIG. 4. Fluxon trajectories in the (υ, X) phase plane for $\Gamma_1 = \Gamma_2 = 0.1$ are plotted to illustrate their dependence on the strength of both the bias current J^B/J_c^o and interband Josephson curent J^{sd}/J^{ss}. Three solid (dashed) curves, from left to right, correspond to $J^B/J_c^o = 0.010$, 0.020 and 0.040 for $J^{sd}/J^{ss} = 0.10$ (-0.10). The vertical dotted lines represent the uniform fluxon speed in the absence of critical current modulation.

and

$$\frac{dX}{d\bar{t}} = \upsilon + \frac{\upsilon - \upsilon^3}{2}\frac{J^{sd}}{J^{ss}}\left(1 - 2\int_0^\infty dy \Upsilon_- \frac{y\,\sinh y}{\cosh^3 y}\right) \quad (67)$$

where $\Upsilon_\pm = \Upsilon_\pm(y,t,X) = \mathrm{sech}^2\alpha_o(\sqrt{1-\upsilon^2}y + X) \pm \mathrm{sech}^2\alpha_o(\sqrt{1-\upsilon^2}y - X)$ and $X = \int_0^{\bar{t}} \upsilon(t')dt' + \bar{x}_o(\bar{t})$. These two equations decribe the fluxon trajectories in the (υ, X) phase plane. We numerically integrate Eqs. (66) and (67) to estimate the fluxon trajectories. The uniform fluxon speed $\upsilon = \upsilon_\infty$ far away from the region of critical current modulation is given by

$$\frac{d\upsilon}{d\bar{t}} = \pm\frac{\pi}{4}\frac{J^B}{J_c^o}(1-\upsilon^2)^{\frac{3}{2}} - \Gamma_1\upsilon(1-\upsilon^2) - \frac{1}{3}\Gamma_2\upsilon. \quad (68)$$

The power-balance velocity υ_∞ may be estimated by setting $d\upsilon/d\bar{t} = 0$. The fluxon speed υ_∞ is obtained by solving the following cubic equation:

$$\sum_{i=0}^{3} a_i z^i = 0\ , \quad (69)$$

where $z = (1-\upsilon_\infty)^{1/2}$, $a_3 = [\pi^2(J^B)^2/16(J_c^o)^2] + \Gamma_1^2$, $a_2 = (2\Gamma_1\Gamma_2/3) - \Gamma_1^2$, $a_1 = (\Gamma_2^2/9) - (2\Gamma_1\Gamma_2/3)$ and $a_0 = -\Gamma_2^2/9$. We note that the solution is bounded by the condition that $0 \le \upsilon_\infty \le 1$ since υ_∞ is given in units of Swihart velocity.

We now estimate the effects of bias current J^B/J_c^o on the fluxon trajectories in the (υ, X) phase plane. In Fig. 4, the fluxon trajectories obtained by numerically integrating Eqs. (66) and (67) are plotted for $J^B/J_c^o = 0.01$, 0.02, and 0.04 (from left to right) to illustrate the position X of the fluxon as a function of velocity υ. Here, we set the dissipation parameters $\Gamma_1 = \Gamma_2$ =0.1. The solid (dashed) curves represent the interband Josephson current density $J^{sd}/J^{ss} = 0.1$ (-0.1). Here, υ_∞ is the uniform initial speed of the fluxon at a position far away from the region of 2π-phase texture which is centered at $X = 0$. The value of υ_∞ depends on J^B/J_c^o. The curve for each J^B/J_c^o shows that, as the fluxon approaches $X = 0$, the fluxon speed deviates from a straight vertical dotted line representing a uniform speed in the absence of the critical current modulation. The curves also show that when the bias current is small (i.e., see, for example, $J^B/J_c^o = 0.010$) the fluxon becomes almost pinned since the pinning effects of the critical current modulation reduce the fluxon speed close to zero. For $J^B/J_c^o < 0.100$, the fluxon is pinned: $\upsilon = 0$ at $X \approx 6.5$ for $J^{sd}/J^{ss} = 0.10$ and $X \approx -6.5$ for $J^{sd}/J^{ss} = -0.10$. However, for $J^B/J_c^o > 0.010$, the fluxon is not pinned since the driving force due to the bias current is larger than the pinning force. The fluxon, approaching from $X = -\infty$, undergoes a notable change in its speed in the region of the critical current modulation. The difference between the maximum and minimum value of the fluxon speed becomes reduced with the increasing bias current density. This is due to that the importance of the pinning effect decreases with increasing value of υ_∞ (i.e., increasing J^B/J_c^o).

As its speed decreases, the fluxon radiates EM waves in the region of critical current modulation. A variation in the fluxon sped may be seen easily in Fig. 4 as a deviation of the fluxon trajectories from the vertical dotted lines. For the solid lines representing the S_{++} symmetry (i.e., $J^{sd}/J^{ss} > 0$), the fluxon speed $\upsilon \ge \upsilon_\infty$ for $X < 0$, but $\upsilon \le \upsilon_\infty$ for $X > 0$. On the other hand, for the dashed lines representing the S_{+-} symmetry (i.e., $J^{sd}/J^{ss} < 0$), the fluxon speed $\upsilon \le \upsilon_\infty$ for $X < 0$, but $\upsilon \ge \upsilon_\infty$ for $X > 0$. The deviation from the uniform fluxon speed υ_∞ increase with the interband Josephson current density $|J^{sd}/J^{ss}|$. This non-uniform fluxon speed due to the critical current modulation suggests that the fluxon absorbs energy from the interband Josephson current to increase the speed from υ_∞, but it returns the energy back to the junction by radiating EM waves, resulting the decrease in the speed.

As suggested by the fluxon trajectories in the (υ, X) phase plane, the bias current density must be larger than the threshold value J_{th}^B in order for the fluxon to pass through the region of critical current modulation. In Fig. 5, we plot the I-V curve for $J^{sd}/J^{ss} = 0.10$ (dotted line) and 0.20 (solid line) to illustrate the dependence of the threshold bias current J_{th}^B on the interband Josephson current (J^{sd}/J^{ss}). The fluxon speed, according to the AC Josephson effect $(1/i)(\partial\varphi/\partial t) = V$, is proportional to the voltage V across the junction. Here, we set the dissipation parameters as $\Gamma_1 = \Gamma_2 = 0.1$ for concreteness. The value of the threshold bias current J_{th}^B for a fixed J^{sd}/J^{ss} may be estimated easily since the voltage across the LJJ does not appear until the bias current reaches the threshold value. The curves show that the threshold bias

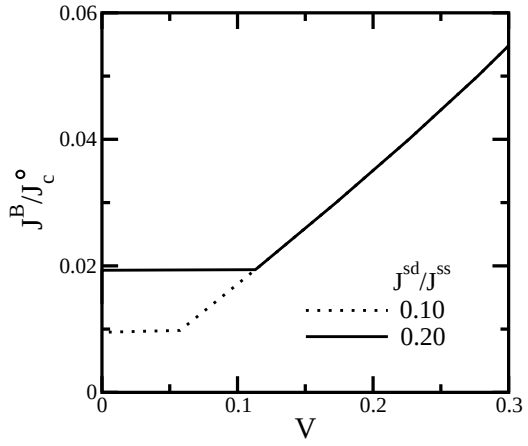

FIG. 5. The current-voltage curves for $J^{sd}/J^{ss} = 0.10$ (dotted line) and 0.20 (solid line) illustrate the dependence of the threshold bias current (i.e., the value of J^B/J_c^o for $V = 0$) on the interband Josephson current. Here, the dissipation parameters are $\Gamma_1 = 0.10$ and $\Gamma_2 = 0.10$.

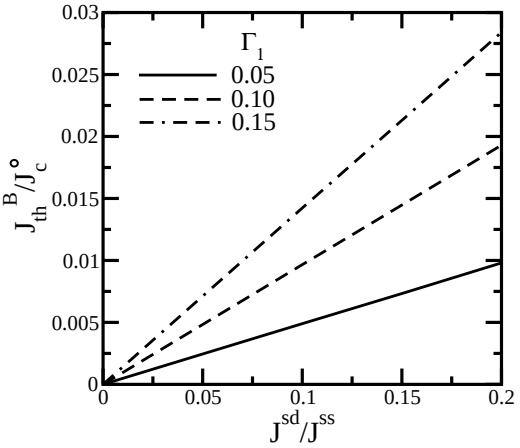

FIG. 6. The threshold bias crrent density J_{th}^B/J_c^o is plotted as a function of J^{sd}/J^{ss} for $\Gamma_1 = 0.05$ (solid line), 0.10 (dashed line) and 0.15(dot-double dashed line) to illustrated the minimum bias current needed to overcome the pinning effect of the critical current modulation. Here, $\Gamma_2 = 0.10$.

current increases with J^{sd}/J^{ss}. As the critical current modulation plays the role of an effective potential for the fluxon, a larger J^B/J_c^o is needed to overcome the pinning effect as J^{sd}/J^{ss} increases. Hence the threshold bias current is similar to the minimum current density needed to overcome the pinning force. In Fig. 5, for $J^B > J_{th}^B$, the I-V curves show that the voltage increases steadily with increasing J^B because the boundary effects are not included in this work. The zero-field step resonances due the boundary current[28] (i.e., a rapidly vanishing critical current near the edges of the junction) are expected to be present along with a smooth increase shown in Fig. 5 when the boundary effects are included.

In Fig. 6, we plot J_{th}^B/J_c^o as a function of J^{sd}/J^{ss} for $\Gamma_1 = 0.05$ (solid line), 0.10 (dashed line) and 0.15 (dot-double dashed line) to illustrate the dependence of the treshold bias current on the interband Josephson effect. We set $\Gamma_2 = 0.10$ for concreteness, but the curves are independent of the strength of the parameter Γ_2. The curves show that J_{th}^B increases linearly with the interband Josephson current J^{sd}/J^{ss}. As indicated by the fluxon trajectories in the (v, X) phase plane, the J_{th}^B/J_c^o versus J^{sd}/J^{ss} curves for both $J^{sd}/J^{ss} > 0$ and $J^{sd}/J^{ss} < 0$ are identical. This indicates that the symmetry of order parameter (i.e., S_{++} versus S_{+-}) may not be distinguished directly from the I-V curves. The increase in the threshold bias current with increasing interband Josephson current implies that, as the critical current modulation increases, a greater strength of driving force must be provided by the bias current to allow the fluxon to pass through the region of a static 2π-phase texture.

VI. SUMMARY AND CONCLUSION

In summary, we have investigated the effects of interband Josephson current on the fluxon dynamics of a LJJ with two-gap superconductors. Due to the multicomponent nature of superconducting order parameter, a 2π-phase texture may be present in each S layer. Accounting for the charge imbalance between the two electronic bands, say s and d bands, we found that the dynamics of the relative phase of the s and d condensates may be described by the equation of motion which is simiar to that for the fluxon. However, the kink-solution for the relative phase (i.e., i-soliton) differs from that for the fluxon. Unlike fluxon, an i-soliton does not carry a magnetic flux quantum but leads to both spatial and temporal modulation of the critical current density.

The critical current density modulation, induced by excitation of an i-soliton representing a 2π-phase texture, behaves as an effective pinning potential for fluxon and modifies the fluxon trajectories. These trajectories in the velocity-position phase plane are similar to those for fluxon moving in the presence of a single microresistor. Moreover, similar to an array of microresistors in the insulator layer of a LJJ, a periodic modulation of the critical current may be created when a spatially periodic array of i-solitons is excited. This critical current modulation can change the fluxon speed when the bias current is applied across the junction in a dissipative environment. In the region far away from the critical current modulation, the fluxon motion is uniform. However, in the region of ciritical current modulation, the fluxon speed can either decrease or increase from the uniform speed as the fluxon either recieves or returns energy to the junction. The decrease in the fluxon speed due to excitation of an i-soliton results in emission of EM radiation (i.e., quasi-linear plasma wave).

The changes in the fluxon speed due to critical current modulation may be reflected in the I-V characteristics. When the bias current is less than the critical value, the fluxon becomes trapped and its speed will be reduced to zero, resulting zero voltage across the junction. This is similar to a fluxon trapped by a microresistor in the I layer. The result suggests an interesting possibility that a double-well potential for a fluxon, which is a necessary condition for a Josephson vortex quantum bit, may be created by exciting two i-solitons in each S layer of the LJJ, rather than implanting two closely spaced microresistors.[35] Also, the I-V curves reveal the dependence of fluxon motion on the bias current. The threshold bias current needed for the fluxon to overcome the critical current modulation appears as a discontinuous jump in the I-V curve at V=0. Hence, this discontinuity may serve as a way to verify the excitation of an i-soliton. Since the size of this discontinuity depends on the interband Josephson current, the I-V curves may be used to estimate the strength of the interband Josephson effect. However, the I-V curves for both the S_{++} and S_{+-} symmetry superconductors are expected to be similar since the threshold bias current does not depend on the symmetry of order parameter.

The present work indicates that the changes in the fluxon dynamics due to excitation of an i-soliton in a single LJJ may become amplified in a multiple LJJ stack where the collective motion of fluxon is known to arise.[36] Also, as recent studies of three-band superconductors indicate, excitation of i-solitons[37] which break[38] the time reveral symmetry is possible when the interband Josephson couplings are frustrated.[39] The fluxon dynamics of a LJJ with three band superconductors may lead to an interesting junction property than that described in the present work.

This work was supported in part by NSF through ND EPSCoR Grant number EPS-081442. The authors would like to thank W. Schwalm for helpful discussions.

APPENDIX:

DERIVATION OF GINSBERG-LANDAU ENERGY FOR A TWO-GAP SUPERCONDUCTOR

For completeness, we derive the Ginsberg-Landau free energy from the two-gap Hamiltonian $\hat{\mathcal{H}}_{TB}$ of Eq. (1) by writing the partition function $\mathcal{Z}$ as

$$\mathcal{Z} = \int \mathcal{D}[\bar{c}^s, c^s]\mathcal{D}[\bar{c}^d, c^d] e^{-\mathcal{S}[\bar{c}^s, c^s, \bar{c}^d, c^d]} \tag{70}$$

where the action $\mathcal{S}$ is given by

$$\mathcal{S} = \int_0^\beta d\tau \Big[\sum_{i,\mathbf{k},\sigma} \bar{c}^i_{\mathbf{k},\sigma} \partial_\tau c^i_{\mathbf{k},\sigma} + \hat{\mathcal{H}}_{TB} \Big] , \tag{71}$$

$\partial_\tau = \partial/\partial\tau$ and $\bar{c}^i_{\mathbf{k}\sigma}$ ($c^i_{\mathbf{k}\sigma}$) is the Grassmann variable representing the creation (annihilation) operator for the i-band electron in the ($\mathbf{k}\sigma$) state. Here, we suppress the S layer index ℓ, for simplicity. We proceed by introducing Nambu notation of $\bar{\mathcal{C}}^i_{\mathbf{k}} = (\bar{c}^i_{\mathbf{k}\uparrow} c^i_{-\mathbf{k}\downarrow})$ and by writing the pair fields $\bar{\mathcal{A}}^i_{\mathbf{k}}$ and $\mathcal{A}^i_{\mathbf{k}}$ as

$$\bar{\mathcal{A}}^i_{\mathbf{k}} = \bar{\mathcal{C}}^i_{\mathbf{k}} \tau_+ \mathcal{C}^i_{\mathbf{k}} = \bar{c}_{\mathbf{k}\uparrow} \bar{c}_{-\mathbf{k}\downarrow} \tag{72}$$

$$\mathcal{A}^i_{\mathbf{k}} = \bar{\mathcal{C}}^i_{\mathbf{k}} \tau_- \mathcal{C}^i_{\mathbf{k}} = c_{-\mathbf{k}\downarrow} c_{\mathbf{k}\uparrow} \tag{73}$$

where $\tau_\pm = (\tau_1 \pm i\tau_2)/2$ and τ_i are Pauli matrices. The action $\mathcal{S}$ of Eq. (71) may be rewritten as

$$\mathcal{S} = \int_0^\beta d\tau \sum_{i,\mathbf{k}} \Big[\bar{\mathcal{C}}^i_{\mathbf{k}} (\partial_\tau I + \epsilon^a_{\mathbf{k}} \tau_3) \mathcal{C}^i_{\mathbf{k}} + \sum_{j,\mathbf{k}'} V_{ij} \bar{\mathcal{A}}^i_{\mathbf{k}} \mathcal{A}^j_{\mathbf{k}'} \Big]. \tag{74}$$

We introduce the Hubbard-Stratonovich transformation to map the interacting system to non-interacting fermions moving in an Hubbard-Stratonovich field Φ (i.e., auxilary field) representing electron pairing. We rewrite the partition function of Eq. (70) as

$$\mathcal{Z} = \int \mathcal{D}[\bar{\mathcal{C}}, \mathcal{C}]\mathcal{D}[\bar{\Phi}, \Phi] e^{-\mathcal{S}[\bar{\mathcal{C}}, \mathcal{C}, \bar{\Psi}, \Psi]} \tag{75}$$

where the action $\mathcal{S}$ is given by

$$\mathcal{S} = \int_0^\beta d\tau \Big[\sum_{i,\mathbf{k}} \bar{\mathcal{C}}^i_{\mathbf{k}} (\partial_\tau I + \epsilon^i_{\mathbf{k}} \tau_3) \mathcal{C}^i_{\mathbf{k}} + \sum_{\mathbf{k},\mathbf{k}'} \Big(\bar{\Phi}_{\mathbf{k}} \frac{1}{V} \Phi_{\mathbf{k}'} - \bar{\mathcal{A}}_{\mathbf{k}} \frac{1}{V} \mathcal{A}_{\mathbf{k}'} \Big) \Big]. \tag{76}$$

Here, we note that $\bar{\Phi}_{\mathbf{k}} = (\bar{\Phi}^s_{\mathbf{k}}, \bar{\Phi}^d_{\mathbf{k}})$, $\bar{\mathcal{A}}_{\mathbf{k}} = (\bar{\mathcal{A}}^s_{\mathbf{k}}, \bar{\mathcal{A}}^d_{\mathbf{k}})$, and V denotes the pairing interaction matrix

$$V = \begin{pmatrix} V_{ss} & V_{sd} \\ V_{sd} & V_{dd} \end{pmatrix} . \tag{77}$$

We shift the Φ field (i.e., $\bar{\Phi}_{\mathbf{k}} \to \bar{\Phi}_{\mathbf{k}} + \bar{\mathcal{A}}_{\mathbf{k}} V$ and $\Phi_{\mathbf{k}} \to \Phi_{\mathbf{k}} + V\mathcal{A}_{\mathbf{k}}$) and obtain

$$\mathcal{S} = \int_0^\beta d\tau \Big[\sum_{i,\mathbf{k}} \bar{\mathcal{C}}^i_{\mathbf{k}} (\partial_\tau I + \epsilon^i_{\mathbf{k}} \tau_3) \mathcal{C}^i_{\mathbf{k}} + \sum_{\mathbf{k},\mathbf{k}'} \Big(\bar{\Phi}_{\mathbf{k}} \frac{1}{V} \Phi_{\mathbf{k}'} + \bar{\mathcal{A}}_{\mathbf{k}} \Phi_{\mathbf{k}'} + \bar{\Phi}_{\mathbf{k}} \mathcal{A}_{\mathbf{k}'} \Big) \Big]. \tag{78}$$

We integrate out the fermion variables $\bar{\mathcal{C}}$ and $\mathcal{C}$ by using the Grassmann integrals and obtain

$$\mathcal{S} = \int_0^\beta d\tau \sum_{\mathbf{k},\mathbf{k}'} \Big[\sum_i \frac{\bar{\Phi}^i_{\mathbf{k}} \Phi^i_{\mathbf{k}'}}{g_i} - \frac{g_{sd}}{g_s g_d} (\bar{\Phi}^s_{\mathbf{k}} \Phi^d_{\mathbf{k}'} + \bar{\Phi}^d_{\mathbf{k}} \Phi^s_{\mathbf{k}'}) \Big] - \mathrm{Tr} \ln G_s^{-1} - \mathrm{Tr} \ln G_d^{-1} \tag{79}$$

where $g_i = (V_{ss}V_{dd} - V_{sd}^2)/V_{ii}$ and $g_{sd} = V_{sd}(V_{ss}V_{dd} - V_{sd}^2)/(V_{ss}V_{dd})$. We note that the first term in Eq. (79)

may be considered as the pesudo-order parameter contribution $\mathcal{S}_{gap}$ to the action. The interacting Green function G_i for the i-band electron is given by

$$G_i^{-1} = (G_i^o)^{-1} + \Sigma_i \tag{80}$$

where the non-interacting Green function G_i^o is given by

$$(G_i^o)^{-1} = \begin{pmatrix} \partial_\tau + \epsilon_{\mathbf{k}}^i & 0 \\ 0 & \partial_\tau - \epsilon_{\mathbf{k}}^i \end{pmatrix} , \tag{81}$$

and the pair interaction Σ_i is given by

$$\Sigma_i = \begin{pmatrix} 0 & \Phi_{\mathbf{k}}^i \\ \bar{\Phi}_{\mathbf{k}}^i & 0 \end{pmatrix} . \tag{82}$$

We may simplify Eq. (79) by expanding the terms $\mathrm{Tr}\ln G_i^{-1}$ as

$$\ln G_i^{-1} = \ln(G_i^o)^{-1} - \sum_{n=1}^{\infty} \frac{(-1)^n}{n} (G_i^o \Sigma_i)^n. \tag{83}$$

In the expansion, all odd order terms vanish when the trace of $\ln G_i^{-1}$ is taken. Assuming that the pair field $\Phi_{\mathbf{k}}^i$ is uniform, we may write the fourth-order contribution in the expansion of $\ln G_i^{-1}$ as

$$\begin{aligned} \frac{1}{\beta}\mathrm{Tr}(G_i^o\Sigma_i)^4 &= \frac{1}{\beta}\sum_\nu \int \frac{d^3\mathbf{k}}{(2\pi)^3} \frac{2|\Phi^i|^4}{[\omega_\nu^2 + (\epsilon_{\mathbf{k}}^i)^2]^2} \\ &= \frac{7\zeta(3)\rho_i}{4\pi^2 T^2}|\Phi^i|^4 \end{aligned} \tag{84}$$

by making the high density approximation. Here, $\omega_\nu = (2\nu+1)\pi/\beta$ with $\nu = 0, \pm1, \pm2, \cdots$ denotes the Matsubara frequency, and $\zeta(x)$ is the zeta-function The second order contribution to the expansion yields

$$\frac{1}{\beta}\mathrm{Tr}(G_i^o\Sigma_i)^2 = \frac{2}{\beta}\sum_{\nu,\mathbf{k},\mathbf{k}'} \frac{|\Phi_{\mathbf{k}-\mathbf{k}'}^i|^2}{(i\omega_\nu - \epsilon_{\mathbf{k}}^i)(i\omega_\nu + \epsilon_{\mathbf{k}'}^i)}. \tag{85}$$

We may simplify the calculation by introducing new momentum variables: $\mathbf{p} = (\mathbf{k}+\mathbf{k}')/2$ and $\mathbf{q} = \mathbf{k} - \mathbf{k}'$. We make a Taylor expansion in $\mathbf{q}$ up to second order, in the high-density limit, and obtain

$$\begin{aligned} \frac{1}{\beta}\mathrm{Tr}(G_i^o\Sigma_i)^2 = \frac{2}{\beta}\sum_{\nu,\mathbf{q}} |\Phi_{\mathbf{q}}^i|^2 \sum_{\mathbf{p}} \Bigg\{ &\frac{1}{\omega_\nu^2 - (\epsilon_{\mathbf{p}}^i)^2} \\ &+ \frac{\mathbf{p}^2\mathbf{q}^2}{12(m_i^o)^2}\left[\frac{-3}{(\omega_\nu^2 + (\epsilon_{\mathbf{p}}^i)^2)^2} + \frac{4(\epsilon_{\mathbf{p}}^i)^2}{(\omega_\nu^2 + (\epsilon_{\mathbf{p}}^i)^2)^3}\right]\Bigg\}. \end{aligned} \tag{86}$$

Here, we used the dispersion relation of $\epsilon_{\mathbf{k}}^i = \mathbf{k}^2/2m_i^o$, where m_i^o is the band mass of the electron. Also we used the relation $p_i p_j \to \delta_{ij}p^2/3$ when the angular average is performed. In Eq. (86), the first term yields the quadratic term (i.e., $|\Phi^i|^2$) in the GL free energy, while the second term of leads to the gradient part of the quadratic term (i.e., $|\nabla\Phi^2|^2$). Combining these terms, we obtain

$$\begin{aligned} \frac{1}{\beta}\mathrm{Tr}(G_i^o\Sigma_i)^2 = &-2\rho_i \ln\frac{2\beta\Lambda e^\gamma}{\pi}|\Phi^i|^2 \\ &+ \frac{7\zeta(3)k_F^2\beta^2\rho_i}{24(m_i^o)^2\pi^2}\int d^3\mathbf{r}|\nabla\Phi^i(\mathbf{r})|^2 \end{aligned} \tag{87}$$

where Λ is the cut-off energy for the boson which mediates pairing interaction and $\gamma \approx 0.5772$. Here, we approximated that $p^2 \approx k_F^2$. We now combine the result and write the coeffcients to the GL free energy expansion for $\bar{\mathcal{G}}_{OB}^i = \mathcal{G}_{OB}^i - \mathcal{G}_{ng}^i$ for one-dimension in the superconducting state as

$$\bar{\mathcal{G}}_{OB}^i = a_i^{GL}|\Phi^i|^2 + \frac{b_i^{GL}}{2}|\Phi^i|^4 + \frac{1}{2m_i^*}\left|\frac{d\Phi^i}{dx}\right|^2 , \tag{88}$$

where the coefficients of the expansion are

$$a_i^{GL} = \frac{1}{g_i} - \rho_i \ln\frac{2\beta\Lambda e^{-\gamma}}{\pi}, \tag{89}$$

$$b_i^{GL} = \frac{7\zeta(3)\beta^2\rho_i}{16\pi^2}, \tag{90}$$

and the effective mass m_i^* is

$$m_i^* = \frac{24(m_i^o)^2\pi^2}{7\zeta(3)k_F^2\rho_i} . \tag{91}$$

The GL free energy of Eq. (88) may be used to estimate the interband phase dynamics by noting that the Hubbard-Strotonovich field may be express in terms of modulus-phase variables as $\Phi_i = |\Phi^i|\exp(i\theta^i)$, as discussed in Sec. III.

[1] H. Ogino, Y. Matsubara, Y. Katsura, K. Uchiyama, S. Horii, K. Kishio, J. Shimoyama, Supercond. Sci. Technol. **22**, 075008 (2009).

[2] H. Suhl, B. T. Matthias and L. R. Walker, Phys. Rev. Lett. **3**, 552 (1959).

[3] A. J. Leggett, Prog. Theor. Phys. **36**, 901 (1966).

[4] A. Liu, I. I. Mazin and J. Kortus, Phys. Rev. Lett. **87**, 087005 (2001); H. J. Choi, D. Roundy, H. Sun, M. L. Cohen, and S. G. Louie, Nature (London) **418**, 758 (2002); G. Karapetrov, M. Iavarone, W. K. Kwok, G. W. Crabtree, and D. G. Hinks, Phys. Rev. Lett. **86**, 4374 (2001); F. Giubileo, D. Roditchev, W. Sacks, R. Lamy, D. X. Thanh, J. Klein, S. Miraglia, D. Fruchart, J. Marcus, and Ph. Monod, Phys. Rev. Lett. **87**, 177008 (2001); H. Schmidt, J. E. Za-

sadzinski, K. E. Gray, and D. G. Hinks, Phys. Rev. Lett. **88**, 127002 (2002).
[5] X. X. Xi, Rep. Prog. Phys. **71**, 116501 (2008)
[6] T. Yokoya, T. Kiss, A. Chainani, S. Shin, M. Nohara, and H. Takagi, Science **294**, 2518 (2001).
[7] R. Joynt and L. Tallifer, Rev. Mod. Phys. **74**, 235 (2002).
[8] D. Jerome and H. J. Schulz, Adv. Phys. **51**, 293 (2002); J. Singleton and C. Mielke, Contemp. Phys. **43**, 63 (2002).
[9] E. Bahaev, Phys. Rev. Lett. **89**, 067001 (2002); Nucl. Phys. B**686**, 397 (2004).
[10] G. Blumberg, A. Mialitsin, B. S. Dennis, M. V. Klein, N. D. Zhigadlo, and J. Karpinski, Phys. Rev. Let. **99**, 227002 (2007).
[11] T. K. Ng and N. Nagaosa, Europ. Phys. Lett. **87**, 17003 (2009).
[12] Y. Ota, M. Machida, T. Koyama and H. Matsumoto, Phys. Rev. Lett. **102**, 237003 (2009); Y. Ota, M. Machida and T. Koyama, J. Phys. Soc. Jpn. **78**, 10370 (2009); T. Koyama, Y. Ota, and M. Machida, Physica C**470**, 1481 (2010).
[13] D. F. Agterberg, E. Demler and B. Janko, Phys. Rev. B**66**, 214507 (2002).
[14] Y. Kamihara, T. Watanabe, M. Hirano, and H. Hosono, J. Am. Chem. Soc. **130**, 3296 (2008); M. Rotter, M. Tegel, and D. Johrendt, Phys. Rev. Lett. **101**, 107006 (2008); J. Paglione and R. L. Green, Nature Phys. **6**, 645 (2010); J. Nagamatsu, N. Nakagawa, T. Muranaka, Y. Zenitani, and J. Akimitsu, Nature (London) **410**, 63 (2001); A. Brinkman and J. M. Rowell, Physica C**456**, 188 (2007).
[15] Y. Ota, M. Machida, and T. Koyama, Phys. Rev. B**83**, 060503(R) (2011); *ibid* B**82**, 140509(R) (2010).
[16] H. Bluhm, N. C. Kosnick, M. E. Huber, and K. A. Moler, Phys. Rev. Lett. **97**, 237002 (2006).
[17] Y. Tanaka, Phys. Rev. Lett. **88**, 017002 (2002).
[18] S. V. Kuplevaskhsky, A. N. Omelyanchouk, and Y. S. Yerin, J. Low. Temp. Phys. **37**, 667 (2011).
[19] Y. Tanaka, A. Iyo, K. Tokiwa, T. Watanabe, A. Crisan, A. Sundaresan, and N. Terada, Physica C**470**, 1010 (2010); Y. Tanaka and A. Crisan, Physica B **404**, 1033 (2009).
[20] J. Goryo, S. Soma and H. Matsukawa, Euro. Phys. Lett. **80** 17002 (2007); Y. Tanaka, A. Crisan, D. D. Shivagan, A. Iyo, K. Tokiwa, and T. WAtanabe, Jpn. J. Appl. Phys. **46**, 134 (2007).
[21] L. Luan, O. M. Auslaender, D. A. Bonn, R. Liang, W. N. Hardy, and K. Moler, Phys. Rev. B**79**, 214530 (2009); J. W. Guikema, H. Bluhm, D. A. Bonn, R. Liang, W. N. Hardy, and K. A, Moler, Phys. Rev. B**77**, 104515 (2008).
[22] A. Gurevich and V. M. Vinokur, Phys. Rev. Lett. **90**, 047004 (2003); *ibid* **97**, 137003 (2006).
[23] C. Vanneste, A. Gilabert, P. Sibillot and D. B. Ostrowsky, J. Low Temp. Phys. **45**, 517 (1981).
[24] D. W. McLaughlin and A. C. Scott, Phys. Rev. A**18**, 1652 (1978).
[25] G. S. Mkrtchyan and V. V. Schmidt, Solid State Commun. **30**, 791 (1979).
[26] B. A. Malomed and M. I. Tbribelsky, Phys. Rev. B**41**, 11271 (1990).
[27] A. Sanchez, A. R. Bishop and F. Dominguez-Adame, Phys. Rev. E**49**, 4603 (1994).
[28] See for example, A. V. Ustinov, *Nonlinear Superconductive Electronics and Josephson Devices*, Edited by G. Costabile, S. Pagano, S. Pedersen, and M. Russo (Plenum Press, New York, 1991) p. 315.
[29] S. G. Sharapov, V. P. Gusynin, and H. Beck, Eur. Phys. B**30**, 45 (2002).
[30] V. Ambegaokar, U. Eckern, and G. Schon, Phys. Rev. Lett **48**, 1745 (1982); U. Eckern, G. Schon, and V. Ambegaokar, Phys. Rev. B**30**, 6419 (1984).
[31] M. Machida, T. Koyama, A. Tanaka, and M. Tachiki, Physica (Amsterdam) C**331**, 85 (2000).
[32] A. I. Larkin and Y. N. Ovchinnikov, Phys. Rev. B**28**, 6281 (1983).
[33] L. P. Go'kov, Soviet Phys. JETP **36**, 1364 (1959); S. Nettel, Phys. Rev. B**48**, 13709 (1993).
[34] M. B. Fogel, S. E. Trullinger, A. R. Bishop, and J. A. Krumhansl, Phys. Rev. Lett. **24**, 1411 (1976); Phys. Rev. B**15**, 1578 (1977).
[35] J. H. Kim, R. P. Dhungana and K.-S. Park, Phys. Rev. B**73**, 214516 (2006).
[36] See, for example, J. H. Kim and J. Pokhrel, Physica C**384**, 425 (2003); S. Sakai, P. Bodin, and N. F. Pedersen, J. Appl. Phys. **73**, 2411 (1993).
[37] J. Garaud, J. Carlsträm, and E. Babaev, Phys. Rev. Lett. **107**, 197001 (2011).
[38] V. Stanev and Z. Tešanović, Phys Rev. B**81**, 134522 (2010); D. F. Agterberg, V. Barzykin, and L. P. Gor'kov, Phys. Rev. B**60**, 14868 (1999); Y. Tanaka and T. Yanagisawa, J. Phys. Soc. Jpn. **79**, 114706 (2010).
[39] S.-Z. Lin and X. Hu, LANL arXiv (cond-mat) 1111.3850v1 (2011); J. Garaud, J Carlström, E. Babaev, Phys. Rev. Lett. **107**, 197001 (2011).